Л.Н. Гумилев атындағы Еуразия ұлттық университетінің хабаршысы. Физика. Астрономия сериясы, 2021, том 135, №2, 57-68 беттер
http://bulphysast.enu.kz, E-mail: vest_phys@enu.kz

МРНТИ: **29.27.47**

S.K. Kunakov [1] , A.A. Imash [2]

[1] *Al-Farabi Kazakh National University, Almaty, Kazakhstan*
[1,2] *Satbayev University, Almaty, Kazakhstan*
(E-mail: [1] sandybeck.kunakov@gmail.com, [2] iimash.aigerim@gmail.com)

Monosilane SiH_4 plasma kinetics generated by e-beam and electrons' energy distribution impact on silicon chemical vapor deposition

Abstract: monosilane (SiH_4) chemical kinetics directly depends on the electrons' energy distribution as well as from the initial electrons cloud formation by external source of ionization. In the present paper electrons' energy distribution calculated from Monte Carlo technique coupled with chemical kinetics. The proposed statistical calculations validated by correspondent Boltzmann equation solutions present drastically different picture of chemical kinetics evolution compared with calculations depicted by Maxwell distribution. The electrons transport coefficients are also evaluated in strong electric fields and analyzed with the accent on the rate of useful chemical reactions (directly connected with the formation of chemical vapour deposition controlled and managed by non-Maxwellian electrons energy distribution.

Keywords: electrons energy distribution function-EEDF,monosilanium SiH_4 , Monte Carlo technique, plasma enhanced chemical vapor deposition (PECVD), Boltzmann equation, Maxwell distribution.

DOI: https://doi.org/10.32523/2616-6836-2021-135-2-57-68
Received: 10.03.2021 / **Accepted:** 17.05.2021

Introduction. Plasma enhanced chemical vapour deposition (PECVD) was widely used in several technological devices [1], [2],[3]. There are presented and described the most detailed primary reactions in $SiH_4 : H_2$ plasmas. The formation of chemical bonds and their chemical properties are also described in [4], [5].

Chemical reactions usually choose the way to the equilibrium state resulting output components and the most undesirable form [6],and [7]. Electrons due to its small masses are flexible to the impact and influence of the external electric field which might be applied in several the technological installations [8] and [9],[10]. Chemical vapour deposition (CVD) of silicon has important technological application and solar cells are the major of them are in following studies: [11], and [12],and [13]. Differences and similarities between μc-$Si : H$ and $a - Si : H$ growth reactions are analysed in [1]. Homogeneous pyrolysis of silane [14] and detailed research up to 5 eV of SiH_4 was theoretically studded decomposition of SiH_4 . The mechanism of two following reactions was studied in [15],[16],[17]:

$$SiH_4 \rightarrow SiH_2 + H_2 \tag{1}$$

and

$$SiH_4 \rightarrow SiH_3 + H \tag{2}$$

The chemical reactions rate constants are presented in detail in [7], [17],[18]. However,the rate of chemical reactions should be corrected, especially in plasma with PECVD technologies, where the electrons are incorporated with active species tending to formation key elementary processes applied to thin films micro crystalline silicon thin films. Most of them solved by Monte Carlo simulation technique [14],[19],[6],[20]. It was experimentally confirmed and theoretically shown that the first reaction plays the dominant role. It should be pointed out that unimolecular decomposition of SiH_4

accompanied by ions and excited states formation. However, the plasma phase within which the ions and excited states like SiH_4^+, H^+, H^*, H_2^* were not taken into consideration. The authors of the study analysed the electron-molecule collisions, cluster growth kinetics in dusty in low pressure SH_4 plasma analysed[6],[13].

1. Elementary processes in $SiH_4 + H_2$ plasma

In the present work there is presented following kinetic model of elementary processes:

Table 1 - Elementary processes in $SH_4 + H_2$ plasma, irradiated by electron beam

№	Reactions	Energy(eV)	Type	Ref
R1	$H_2 + e \to H_2 + e$	$3kT_e m_e/m_{(H_2)}$	Elastic H_2	[21][22]
R2	$SiH_4 + e \to SiH_4 + e$	$3kT_e m_e/m_{(SiH_4)}$	Elastic SiH_4	[7][22]
R3	$H_2 + e \to e + 2H$	8.9	Dissoc H_2	[7][21]
R4	$SiH_4 + e \to e + SiH_3 + H$	5.8	Dissoc SiH_3	[21]
R5	$SiH_4 + e \to e + SiH_2 + H_2$	10.9	Dissoc SiH_2	[7][22]
R6	$SiH_4 + e \to e + SiH_2 + 2H$	7.8	Dissoc SiH_2	[7][22]
R7	$SiH_4 + e \to e + SiH + H_2 + H$	16.2	Dissoc SiH	[7]
R8	$SiH_4 + e \to SiH_3^- + H$	6.5-11	Affinity SiH_4	[21][22]
R9	$SiH_4 + e \to e + SiH_4^{\nu 13}$	0.27	Excitation SiH_4	[21]
R10	$SiH_4 + e \to e + SiH_4^{\nu 24}$	0.113	Excitation SiH_4	[21]
R11	$H_2 + e \to H_2^* + e$	11.3	Excitation H_2	21]
R12	$H_2 + e \to H_2^{j02} + e$	0.0453	Excitation H_2	[21][22]
R13	$H_2 + e \to H_2^{j13} + e$	0.0727	Excitation H_2	[21][22]
R14	$H_2 + e \to H_2^{\nu 1} + e$	0.516	Excitation H_2	[21]
R15	$H_2 + e \to H_2^{\nu 2} + e$	1.08	Excitation H_2	[21]
R16	$H_2 + e \to H_2^{\nu 3} + e$	1.5	Excitation H_2	[21]
R17	$H_2 + e \to H_2\left(\sum_{Rydberg}\right) + e_2$	15.2	Excitation H_2	[22]
R18	$H_2 + e \to H_2^+ + 2e$	15.4	Ionization H_2	[21][22]
R19	$SiH_4 + e \to SiH_3^+ + H + 2e$	11.9	Ionization SiH_4	[7][21]
R20	$H_2^+ + 2e + SiH_3^- \to H_2 + SiH_3$	$\approx T$e	Recom H_2	[22]

Cross sections for electrons and hydrogen molecules were taken from [18].

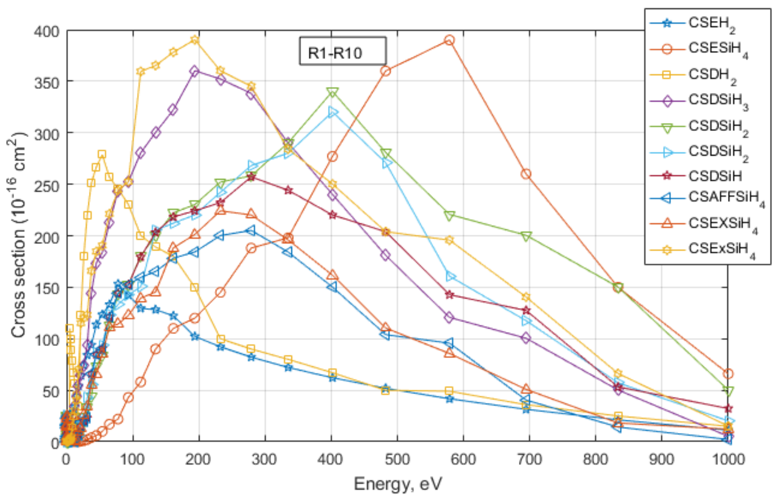

Figure 1 – Cross sections for electron impact reactions for SiH_4 and H_2 from R1 to R10 (table 1)

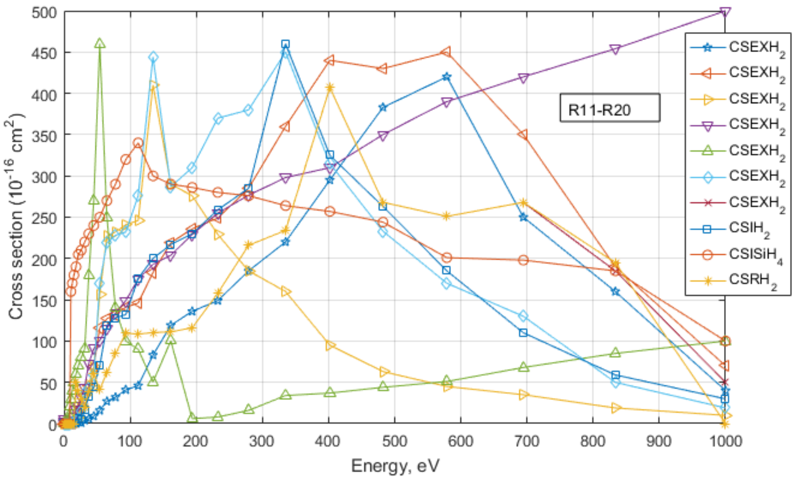

FIGURE 2 – Cross sections for electron impact reactions for SiH_4 and H_2 from R11 to R20 (table 1)

.

The plots corresponding to calculated with data to the cross sections for SiH_4 and H_2 are presented in figure 1 and figure 1, respectively.

2. Boltzmann equation for e-beam

We should enumerate some innovative publication to adjust Boltzmann equation to study formation of micro structural chemical plasma deposition devices and theoretical methods like in [23],[24],[25],[26].Following to the earlier made studies [27],[28],[24],[21] the Boltzmann equation for electron beam in the gas mixture we are presenting in the following way:

$$\partial_e f_e(t,\overrightarrow{r},\overrightarrow{\xi}) = S_e^{eb} + S_e^{pe}(f_e) + S_e^{ion}(f_e) + \sum_k S_{e,k}^{exc}(f_e) + \\ + S_e^{el}(f_e) - \sum_k S_{e,k}^{dis}(f_e) - S_e^{rec}(f_j * f_e) \tag{3}$$

here $f_e(t,\overrightarrow{r},\overrightarrow{\xi})$ is distribution function of electron beam in the $SiH_4 : H_2$ plasma by time, radius vector and velocity. It should be known that the variables t and $\overrightarrow{r}$ are hydrodynamic, but they microscopic variables and the $\overrightarrow{\xi}$ should be considered as the velocity of a particle (fission fragments). $S_e(f_e)$ is the collisional member according to elementary processes.

$$\int_0^{\xi_e^{max}} f_e(t,\overrightarrow{r},\overrightarrow{\xi})\, \mathrm{d}\,\overrightarrow{\xi} = n_e(t,\overrightarrow{r}) \tag{4}$$

here $n_e(t,\overrightarrow{r})$ is concentration of particles in plasma by time and radius vector.

$$\partial_e = \frac{\partial}{\partial t} + \xi_i \frac{\partial}{\partial x_i} + a_i \frac{\partial}{\partial \xi_i}. \tag{5}$$

Equation 5 is an auxiliary mathematical apparatus that includes the characterization of particles in a plasma.

$$f_e^p(t,\overrightarrow{r},\overrightarrow{\xi}) = \int_I^{\xi_{max}} \Omega_j^{ion}(\triangle E_j,\xi_j) f^{eb}(t,\overrightarrow{r},\overrightarrow{\xi}) d(\triangle E_j) \tag{6}$$

Here Ω_j^{ion} is the source j-type of fragments on full differential cross-section for ionization proses, I - is ionization potential, $\triangle E_j$ is energy loss, that is equal an energy received by allocated electron and total amour of ionization potential. Further solution looks like this

$$\int_0^{\infty} \delta(\overrightarrow{\xi} - \overrightarrow{\xi}_e^0)\, \mathrm{d}\,\overrightarrow{\xi} = 1 \tag{7}$$

here $\delta(\overrightarrow{\xi} - \overrightarrow{\xi}_e^0)$ is a delta function that represents at the point of the initial energy a fission fragment by the energy distribution.Based on the above data the energy of the primary electron with the law of conservation of energy for a charged electron has the form of kinetic energy as follows:

$$\varepsilon_e^{esc} = \int_0^{\xi_{max}} f_e^{pe}(t, \overrightarrow{r}, \overrightarrow{\xi}) \frac{m_e \xi^2}{2} d\xi \tag{8}$$

here m_e is effective mass of primary electrons. The function of distribution of electron beam is following:

$$f^{eb} = n_0 \left(\frac{m_e}{E^{eb}} \right)^{\frac{3}{2}} \delta(\xi - \xi_0^{eb}) \tag{9}$$

then we have collisional member for ionization:

$$\begin{aligned} S_e^{ion}(f_e(t, \overrightarrow{r}, \overrightarrow{\xi})) = \sum_k \{ n_k \int_{\xi + \sqrt{\frac{2I_k}{m_e}}}^{\xi_e^{max}} \delta(\xi_j^{'} - G_{e,k}^{ion}(\xi_j^{'}, \xi_j) p_j^{ion}(E_e^{'}) d\xi_e^{'} * \\ * \int_{I_k}^{E_0 - I_k} f_j(\xi_j^{'}) \xi_j^{'} \Omega_{e,k}^{ion}(\xi_e^{'}, \triangle E_e) d(\triangle E_j) - \\ - n_k \int_0^{E_0 - I_k} p_{e,k}^{ion}(E_j) f_e(\xi_e) \xi_e \Omega_{e,k}^{ion}(\xi_e^{'}, \triangle E_e) d(\triangle E_e) \} \end{aligned} \tag{10}$$

Following to [29] and [30] the primary electrons energy distribution equals:

$$\begin{aligned} & f_e^{pe}(\varepsilon) = n_e^0 \left\{ \frac{m_e}{E_q} \right\} * G(\varepsilon) \\ & G(\varepsilon) = \frac{I^3}{(I+\varepsilon)^2 E_q} \left\{ \frac{\frac{I+\varepsilon}{I} + \frac{4}{3}(1 - \frac{I+\varepsilon}{I} Ln(2.7 + (\frac{E_q - I - \varepsilon}{I})^{0.5})}{1 + \frac{1}{3} Ln(2.7 + (\frac{E_q - I}{I})^{0.5}} \right\} \\ & E_q = \frac{m_e (\xi_e^{eb})^2}{2} \end{aligned} \tag{11}$$

here $G(\varepsilon)$ is collision integral of primary electrons, E_q is kinetic energy of primary electrons with hydrodynamical variable by velocity.

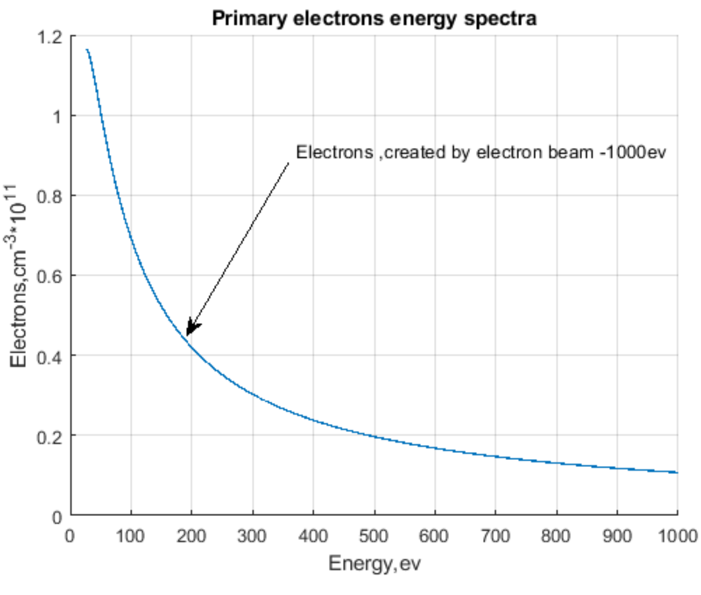

Figure 3 – Primary electrons energy spectra,calculated by formula-(11)

.

From equation we may deduce the hydrodynamical equation for $SiH_4 + H_2$ plasma, irradiated by electron beam:

$$\begin{aligned} &\tfrac{\partial n_e(t,\overrightarrow{r})}{\partial t} + \nabla \overrightarrow{j}_e(t,\overrightarrow{r}) = S_e^{eb}(t,\overrightarrow{r}) + S_e^{pe}(t,\overrightarrow{r}) + k^T(t,\overrightarrow{r})n_e(t,\overrightarrow{r}) - \\ &- k^{aff}(t,\overrightarrow{r})n_e(t,\overrightarrow{r}) - k^{rec}(t,\overrightarrow{r})n_e^2(t,\overrightarrow{r}) \\ &\overrightarrow{j}_e = -D_e \nabla n_e + b_e n_e \overrightarrow{E} - D_e^T \nabla T_e \\ &\nabla \overrightarrow{E} = -4\pi(n_e + n^- - n^+) \end{aligned} \tag{12}$$

$$\frac{\partial}{\partial t}\left\{\frac{3}{2} n_e k T_e\right\} = S^{eb} * E^{eb} - S^{pe} E_e^{av} - \lambda \nabla T_e - \chi(T_e - T_0) \tag{13}$$

This curve (figure 3) can be compared [21] for reasons, the primary electron loses energy or it can be assumed that at the birth of the secondary electron this spectrum decreases, our model places the ionization peak at a slightly higher height more precisely showing the peak at high energy.

3. Electrons Boltzmann equation solution. Time dependent case

We should select three time scale in the evolution of electrons beam energy to local Maxwellian distribution. The first one, the fast time scale lasts from zero to $10^{-11}sec$ - $10^{-9}sec$ [31] and connected with the fast transformation of mono energetic electrons energy of the electrons beam to the formation of primary electrons energy spectra and exciting neutrals of the testing gas. The second time scale is the slow time scale and it will be characterized by small parameter ϵ, which is to

$$\varepsilon = \delta \sqrt{\frac{E_{av}^e}{E_q}}, \quad \delta = \frac{m_e}{M} \tag{14}$$

here M, m $_e aremasscollidingatom's.Therelationbetweenthesetwoscalesisasfollows: t^{slow\ scale} = \frac{t^{fast\ scale}}{\varepsilon}$(15) The third time scale is slower than the second one and rings the local Maxwellian energy distribution related with the further transformation electrons energy to heating neutrals and recombination and affinity processes. The relation of the slow elastic degradation and its corresponds to the very slow time scale last around $10^{-9}sec$ till $10^{-7,-3}sec$ and related with the first fast time scale as follows:

$$t^{maxwellization} = \tfrac{t^{fast\ scale}}{\varepsilon^2} \tag{16}$$

So, we may present these three types of energy distribution function as the following series:

$$\frac{\partial f_e(t,\xi)}{\partial t} = \left(\frac{\partial f}{\partial t}\right)^{(0)} + \varepsilon\left(\frac{\partial f}{\partial t}\right)^{(1)} + \varepsilon^2\left(\frac{\partial f}{\partial t}\right)^{(2)} + ... \tag{17}$$

For quick, slow and Maxwellian time relaxation we may present The Boltzmann equation slitted into three equation:

$$\left(\tfrac{\partial f}{\partial t}\right)^{(0)} = S^{eb}(t,\xi_0(t)) + n_e^{eb}\left(\tfrac{m_e}{E^{eb}}\right)^{\frac{3}{2}} \int_\xi^{\xi_0} \int_I^{E^{eb}} \Omega^{ion}(\triangle E \xi')\delta(\xi' - \xi_0) d(\triangle E)$$

$$*\delta(\xi - G^{ion}(\xi',\xi))\xi' d\xi' - n_e^{eb}\left(\tfrac{m_e}{E^{eb}}\right)^{\frac{3}{2}} \int_I^{E^{eb}} \Omega^{ion}(\triangle E,\xi)\xi f(t,\xi) d(\triangle E)$$

(18)

Over time, electrons from the electron beam are converted into primary electrons, which complete the rapid passage of time. By introducing a deceleration function $G(t)$ we obtain the evolution of the electron energy distribution on this timescale as follows:

$$f^{fast\ scale}(t,\xi) = n_0^e\left(\frac{m_e}{E^{eb}}\right)\delta(\xi - \xi_0) + f^{pe}(\xi) - f^{pe}(\xi)e^{-\frac{t}{\tau}} \tag{19}$$

$$f^{slow\ scale}(t,\xi) = n_0^e \left(\frac{m_e}{E^{eb}}\right)\delta(\xi-\xi_0) + f^{pe}(\xi) - f^{pe}(\xi)e^{-\frac{t}{\tau}} + f^M(\xi) - f^M(\xi)e^{-\frac{t}{\varepsilon\tau_1}}$$
$$f^M(\xi) = n_e\left(\frac{m_e}{kT_e}\right)^{\frac{3}{2}} e^{-\frac{m_e\xi^2}{kT_e}} \quad (20)$$

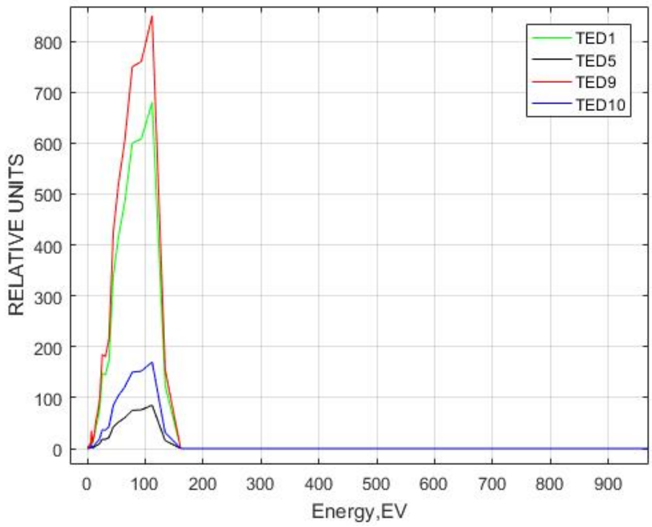

FIGURE 4 – Secondary electrons energy spectra evolution in $SiH_4 : H_2$ plasma, generated by e-beam

.

Monte Carlo simulation allowed us to get the evolution. The secondary electron, the mathematical solution are equations (19) and (20). Figure 4 shows the theoretical calculation obtained by simulation. It shows that the red line corresponds to (TED9=9ns) in the ninth nanosecond time interval and shows that the electron energy has the maximum value in this interval. We considered the ten-time interval for numerical calculation and derived only (TED1=0.1ns, TED5=5ns, TED10=10ns) these intervals in graphical form. In different time intervals, the energy and number of electrons change periodically.

4. Monte Carlo programming code description

The series of works were undertaken to analyse the chemical kinetics in $SiH_4 + H_2$ mixtures by Monte Carlo technique like [7], The programming complex described in the present paper consists of three main parts:initial data input $INDATA$, life history trace of $SiH_4 + H_2$ fragments and electrons degradation spectra in subroutine MKN
and recording all output data $DATAOUT$ in files with intention txt. One of the electron's history in any elementary process starts in subroutine $BEGHIS$. In the case when ff is not the subject of external field their initial energy of the played electron equals to the energy released from e-beam source. Because of the isotropic space distribution the secondary electrons directions are taken randomly. It also should be noted that initial coordinates are taken within a given volume. Intensity of directly connected with neutron flux energy and space distribution of e-beam source. The main program MCN has two loops; first one counts the number of played histories, the second loop traces the electron life history till its energy decreases to the defined minimum limit or crosses the boundaries of the given volume. Within the second loop whatever electron energy is, the integral cross section recalculated and free flight length is defined:

$$R = -\frac{ALOG(CL)}{S}, S = \sum_i N_i\sigma_{ij}(SiH_4, H_2, e) \quad (21)$$

here CL-is random number with equal probability within 0,1, S - is total cross section. If during electron free flight charged particles are not affected by external electric field electrons come to target atom and calculation procedure addresses to the subroutine $ELACT$. In the presence of external field the fission fragments accelerate or lose their energy. In subroutine $ELACT$ one of a number of elementary processes choice is realized by the following rule. The normalized ladder of all possible interactions cross sections corresponding to the current value of fission fragment energy is compiled. Then the successive comparison with random number brings lucky choice for fission fragment or for electron. The block scheme of the programming code is presented below:

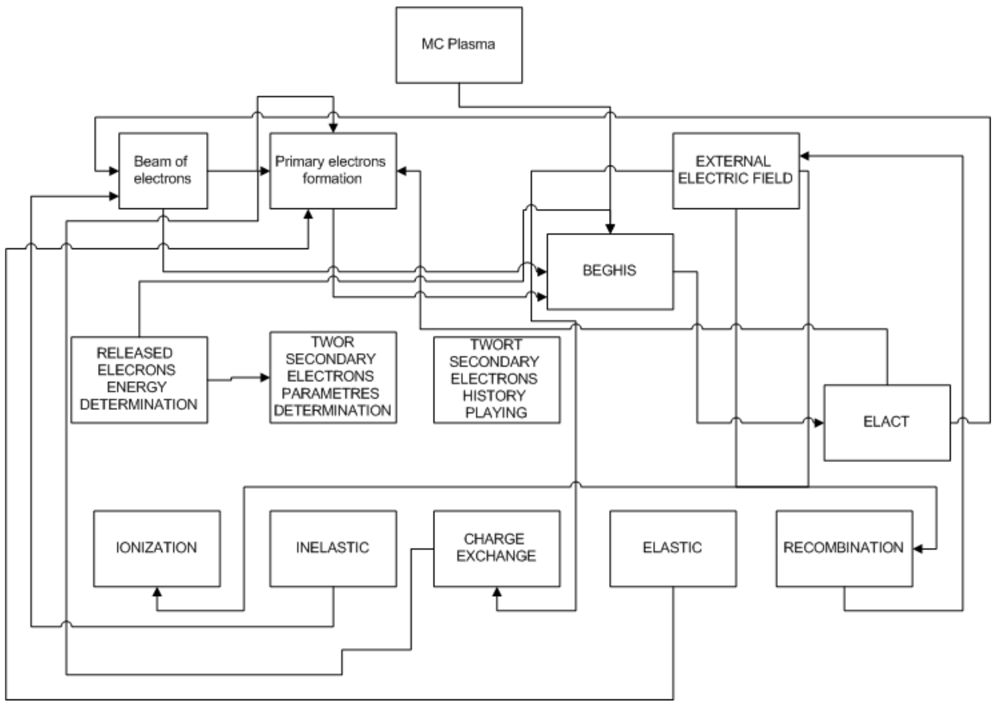

in SiH4.png

Figure 5 – Block diagram of the calculation of the energy spectrum of the e-beam electrons by the Monte Carlo method in the $SIH_4 : H_2$ excited plasma, placed in the core of a stationary electron beam

.

After the elementary process has been chosen the loss of energy, intensity and other collision parameters are booked and returned to the main program (figure 5). In case of three body collision the energy loss of initial particle compiled from three parts. Firstly, recoil loss, secondly, ionization potential and thirdly the energy of third created particle (primary electron) which has sufficiently large range of captured energy from zero up to the total particle energy. Probability of this process inversely proportional to energy loss taken proportional to loss of energy, taken in the negative second power. The subroutines responsible to make these calculations are in $TWOW, TWOR$. The acquired energy of primary electrons as well as other parameters like position coordinates, directions recorded and primary electron's histories successively played as in the fission fragments manner. The calculation code was compiled on the time depending scheme allowing and handling the processing circuits synchronized in the given time intervals and branching process for two and more generations. After each act of ionization created the primary electrons' history (independently of source-heavy fission fragments or born fast primary electron) traced during its full life. The energy of secondary electrons created by primary ones are also randomly played and memorized in queue arrays which then they are used to trace secondary electrons histories by the LIFO rule (last in, first out). There was carried out tracking the trajectories of the primary electron's energy was carried out up to 0.1 eV. Recombination of positive particles, protons and tritium nuclei played and tracked up the thermal region and ends counting in thermal region until all electrons are taken from the present energy distribution of histories of electrons. Integral cross section of recombination needs the total concentration of positive ions in plasma which was calculated from ionization rate and lifetime of the ion's history.

5. Chemical kinetics

The numerical models review [32], [33] shows the vital interest to the formation of of thin film and plasma chemistry around the surface boundaries. However, for the physics of a gas phase, it is often necessary to know the rate of occurrence or death of a particle of a specific sort in the plasma or the rate of reaction flow. The reaction rate refers to the number of elementary acts of birth or death of a particle per unit volume of plasma per unit time. This value is proportional to the concentrations of the particles involved in the reaction. In the future, to denote the concentration of particles, we will enclose the corresponding particle symbol in square brackets.

$$\begin{aligned}&\tfrac{d}{dt}\,[H^+] = k_{11}(t)n_e[H_2] - k_{12}[H^+][SiH_4] - k_{13}[H^+][SiH_3]\\&-k_{14}[H^+][SiH_2] - k_{15}[H^+][SiH]\\&k_{12}(t) = \textstyle\int_0^{\xi_{max}} \sigma^{ion}(\varepsilon)\sqrt{\tfrac{2\varepsilon}{m_e}}f_e(t,\varepsilon)\,\mathrm{d}\,\varepsilon\end{aligned} \tag{22}$$

$$\begin{aligned}&\tfrac{d}{dt}\,[H_1^*] = k_{21}(t)n_e[H_2] - k_{22}[H_1^*][SiH_4] - k_{23}[H_1^*][SiH_3]\\&-k_{24}[H_1^*][SiH_2] - k_{25}[H_1^*][SiH]\\&k_{21}(t) = \textstyle\int_0^{\xi_{max}} \sigma_1^{exc}(\varepsilon)\sqrt{\tfrac{2\varepsilon}{m_e}}f_e(t,\varepsilon)\,\mathrm{d}\,\varepsilon\end{aligned} \tag{23}$$

here σ - is interaction cross-section of electron-atomic collisions in gas-kinetic theory

$$\frac{d}{dt}[H_1^*] = k_{21}n_e[H_2] - k_{22}[H_1^*][SiH_4] \tag{24}$$

$$\frac{d}{dt}[H_2^*] = k_{31}n_e[H_2] - k_{32}[H_2^*][SiH_4] \tag{25}$$

The proportionality coefficients K_1n, K_2n included in these expressions that characterize the collision process are called reaction rate constants. The rate constant of the two-particle process has the dimension K $[cm^2/s]$.

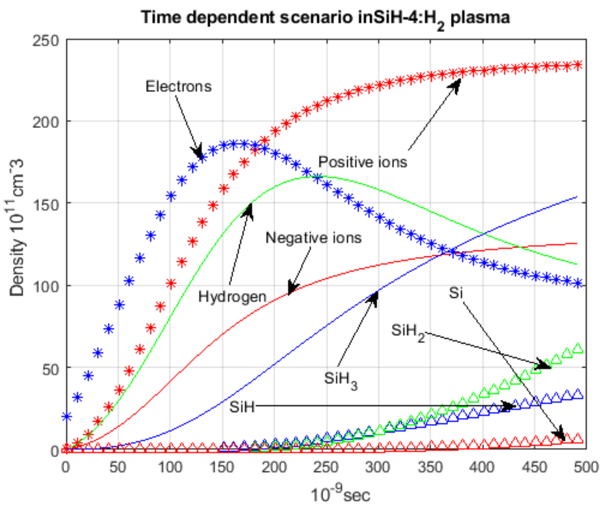

Figure 6 – Chemical kinetics scenario in $SiH_4 : H_2$ plasma, generated by e-beam

.

However the detailed mathematical models describing these diffusion processes and why the species like SiH_3 that play a key role in these processe have not been discussed. Nevertheless we present one of the possible scenario (figure 6) of kinetics evolution in such a plasma taking the kinetics coefficients as functional from electrons energy distribution as a functions dependent from time and energy. Questions about the kinetics at the boundary surface where the crystallizations of microcrystalline silicon $\mu c - Si : H$ and amorphous silicon $a - Si : H$ are beyond the scope of this article.

Conclusions

- There has been defined time dependent solution of Boltzmann kinetic equation solution for electrons function of energy distribution
- There has been developed Monte Carlo technique applied to the simulation of the electron's energy spectra evolution the Maxwellian one
- Relaxation of electrons energy spectra to the local Maxwellian distribution, carried out by the Monte Carlo method, demonstrates a similar time dependence and confirms time dependent solution for electron beam Boltzmann kinetic equation
- Chemical kinetics shows a sharp dependence of ion formation from on time-time dependent electron energy spectra in PECVD technology for $SiH_4 : H_2$ plasmas.

References

1 Matsuda A. Microcrystalline silicon. Growth and device application // Journal of Non-Crystalline Solids. - 2004. - T. 338. - P. 112.

2 Kushner M.J. A model for the discharge kinetics and plasma chemistry during plasma enhanced chemical vapour deposition of amorphous silicon // Journal of applied physics. - 1988. - T. 63. - P. 2532-2551.

3 Wang S. Evolution of a-Si: H to nc-Si: H transition of hydrogenated silicon lms deposited by trichlorosilane using principle component analysis of optical emission spectroscopy // Materials Chemistry and Physics. - 2020. - T. 240. - P. 122-186.

4 Raghunath P Lee Y. Ab initio chemical kinetics for reactions of H atoms with SiH_x (x= 13) radicals and related unimolecular decomposition processes // International Journal of Quantum Chemistry. - 2013. - T. 113. - P. 1735-1746.

5 Nguyen T.N., Lee Y.M. Wu J.S., Lin M.C. Ab Initio Chemical Kinetics for the Thermal Decomposition of SiH_4^+ Ion and Related Reverse Ion Molecule Reactions of Interest to PECVD of a-Si: H Films // Plasma Chemistry and Plasma Processing. - 2017. - T. 37. - P. 1249-1264.

6 Phillip J.S Kushner M.J. Monte Carlo simulation of surface kinetics during plasma enhanced chemical vapour deposition of SiO_2 using oxygen/tetraethoxysilane chemistry // Journal of Vacuum Science Technology A: Vacuum, Surfaces, and Films. - 1993. - T. 11. - P. 2562-2571.

7 Babahani O., Hadjadj S., Khelfaoui F., Kebaili H. O. Lemkeddem S. Monte Carlo simulation of chemical reactions in plasma enhanced chemical vapour deposition: From microscopic view to macroscopic results // Silicon. - 2019. - T. 11. - P. 1267-1274.

8 Balbuena J.P Martin-Bragado I. Lattice kinetic Monte Carlo simulation of epitaxial growth of silicon thin films in H_2/SiH_4 chemical vapour deposition systems // Thin Solid Films. - 2017. - T. 634. - P. 121-133.

9 Da B Lihao Y. Monte Carlo simulation study of reflection electron energy loss spectroscopy of an Fe/Si over layer sample // Surface and Interface Analysis. - 2020. - T. 52. - P. 742-754.

10 Kimberly R.M., Alan L.M., Eduardo D.G. Storage of natural gas by adsorption on activated carbon // Chemical engineering science. - 1992. - T. 47. - P. 1569-1579.

11 Holt J.K., Swiatek M., Goodwin D.G. Harry A.A. Gas Phase and Surface Kinetic Processes in Hot-Wire Chemical Vapour Deposition // Amorphous Heterogeneous Silicon Thin Films. - 2011. – T. 609. – P. 62.

12 Shogo S., Masao S, Hisanao A., Shigeo S. Silicon-Carbon alloy film formation on Si (100) using SiH_4 and CH_4 reaction under low-energy ECR Ar plasma irradiation // Materials Science in Semiconductor Processing. - 2017. - T. 70. – P. 188-192.

13 Kushner M.J. A model for the discharge kinetics and plasma chemistry during plasma enhanced chemical vapour deposition of amorphous silicon // Journal of applied physics. - 1988. - T. 63. - P. 2532-2551.

14 Бенилов М.С. Теория электрических зондов в потоках слабоионизованной плазмы высокого давления // Теплофизика высоких температур, Российская академия наук, Отделение энергетики, машиностроения, механики и ... - 1988. - Т. 26. - С. 993-1004.

15 Kees L., Wim J.G. Ioannis P., Rath K. Ion bombardment measurements and simulations of a low temperature VHF PECVD SiH_4H_2 discharge in the a-Si: H to μc-Si: H transition regime // physics status solidi (a). - 2016. - T. 213. - P. 1680-1685.

16 Timothy J.S. Kushner M.J. Monte Carlo-fluid model of chlorine atom production in Cl_2, HCl, and ﬄCCl_4 radio-frequency discharges for plasma etching // Journal of Vacuum Science Technology B: Microelectronics and Nanometer Structures Processing, Measurement, and Phenomena. - 1992. - T. 10. - P. 2179-2187.

17 Marvi Z., Xu S., Foroutan G., Ostrikov K. Levchenko I. Plasma-deposited hydrogenated amorphous silicon films: multi scale modelling reveals key processes // RSC advances. - 2017. - T. 7. - P. 19189-19196.

18 Tawara H., Itikawa Y., Nishimura H. Yoshino M. Cross sections and related data for electron collisions with hydrogen molecules and molecular ions // Journal of Physical and Chemical Reference Data. - 1990. - T. 19. - P. 617-636.
19 Timothy J.S. Monte Carlo-fluid hybrid model of the accumulation of dust particles at sheath edges in radio-frequency discharges // Applied physics letters. - 1991. - T. 59. - P. 638-640.
20 Sasa D., Zoran M.R., Ronald D.W., Toshiaki M. Zoran L.P. Monte Carlo analysis of ionization effects on spatio-temporal electron swarm development // The European Physical Journal D. - 2014. – T. 68. – P. 166.
21 Zhang B. Zhang X. Electron energy distribution functions relevant for weakly ionized SiH_4H_2 plasma // Journal of Physics D: Applied Physics. - 2020. - T. 53. - P. 115-201.
22 Jason P. Modeling and Experimental process optimization for a $SiH_4 + H_2$ surface wave plasma discharge for silicon photovoltaic. - 2014.
23 Grari M. and Zoheir C. Numerical Modeling of Non-equilibrium Plasma Discharge of Hydrogenated Silicon Nitride ($SiH_4/NH_3/H_2$) // International Journal of Engineering. - 2020. - T. 33. - P. 1440-1449.
24 Hagelaar G.J. Pitchford L.C. Solving the Boltzmann equation to obtain electron transport coefficients and rate coefficients for fluid models // Plasma Sources Science and Technology. - 2005. - T. 14. - P. 722.
25 Oblapenko G., Goldstein D., Varghese P. Moore C. A velocity space hybridization-based Boltzmann equation solver // Journal of Computational Physics. - 2020. - T. 408. - P. 109-302.
26 Mohammad M.O., Saeed R.H. Boltzmann equation studies on electron swarm parameters for oxygen plasma by using electron collision cross sections // Zanco Journal of Pure and Applied Sciences. - 2020. - T. 32. - P. 36-53.
27 Chapman S., Thomas G.C. David B. The mathematical theory of non-uniform gases: an account of the kinetic theory of viscosity, thermal conduction and diffusion in gases. - Cambridge: Cambridge university press, 1990. - 423 p.
28 Holstein T. Energy distribution of electrons in high frequency gas discharges // Physical Review - 1946. - T. 70. - P. 367.
29 Gryzinski M. Classical theory of atomic collisions. I. Theory of inelastic collisions // Physical Review. - 1965. - T. 138. - P. A336.
30 Guyot J., Miley G. Verdeyen J. Application of a two-region heavy charged particle model to Noble-gas plasmas induced by nuclear radiations // Nuclear Science and Engineering. - 1972. - T. 48. - P. 373-386.
31 Tsendin L. The electron diffusion coefficient in energy in bounded collisional plasmas // IEEE transactions on plasma science. - 2006. - T. 34. - P. 728-737.
32 Bogaerts A., Eckert M., Mao M., Neyts E. Computer modelling of the plasma chemistry and plasma-based growth mechanisms for nano structured materials // Journal of Physics D: Applied Physics. - 2011. - T. 44. - P. 174030.
33 King H., Pflug A., Ortner K., Hofer M., Harig T., Sittinger V. DSMC - Simulation of the influence of hydrogen addition on the properties of silicon deposited by HWCVD // Surface and Coatings Technology. - 2019. - T. 379. - P. 125035.

С.К. Кунаков [1] , А.А. Имаш [2]

[1,2] *Әл-Фараби атындағы Қазақ ұлттық университеті, Алматы, Қазақстан*
[2] *Қ.И.Сәтпаев атындағы Қазақ Ұлттық Техникалық Зерттеу Университеті, Алматы, Қазақстан*

Электронды сәуле арқылы шығарылған моносилан плазмасының SiH_4 кинетикасы және электрон энергиясының таралуының кремнийдің бу фазасыда тозаңдануына әсері

Аннотация. Моносиланның химиялық кинетикасы SiH_4 тікелей электрон энергиясының таралуына, сонымен қатар сыртқы иондану көзі арқылы электрон бұлтының пайда болуына тікелей байланысты. Бұл жұмыста электронды энергияның таралуы Монте-Карло әдісімен химиялық кинетикамен ұштастыра есептеледі. Больцман теңдеулерінің сәйкес шешімдерімен расталған ұсынылған статистикалық есептеулер Максвелл үлестірімімен салыстырғанда химиялық кинетика эволюциясының мүлдем басқа көрінісін білдіреді. Электрондардың берілу коэффициенттері күшті электр өрістерінде де бағаланады және пайдалы химиялық реакциялардың жылдамдығына баса назар аударылады және химиялық будың тұндыруымен тікелей байланысты, басқарылатын және бақыланатын Максвеллианнан тыс электрондар энергиясы.

Түйін сөздер: электрондардың энергия бойынша таралу функциясы-ЭЭТФ, моносилан SiH_4 , Монте-Карло әдісі, бу фазасында химиялық қондыру (PECVD), Больцман теңдеуі, Максвелл таралуы.

С.К. Кунаков [1] , А.А. Имаш [2]

[1,2] *Национальный университет им. Аль-Фараби, Алматы, Казахстан*
[2] *Казахский национальный исследовательский технический университет им. К.И. Сатпаева, Алматы, Казахстан*

Кинетика плазмы моносилана SiH_4 , генерируемой электронным пучком, и влияние распределения энергии электронов на химическое осаждение кремния из паровой фазы

Аннотация. Химическая кинетика моносилана SiH_4 напрямую зависит от распределения электронов по энергиям, а также от образования исходного облака электронов внешним источником ионизации. В данной статье распределение электронов по энергиям рассчитывается методом Монте-Карло в сочетании с химической кинетикой. Предлагаемые статистические расчеты, подтвержденные соответствующими решениями уравнения Больцмана, представляют

кардинально иную картину эволюции химической кинетики по сравнению с той, которая изображена распределением Максвелла. Коэффициенты переноса электронов также оцениваются в сильных электрических полях и анализируются с акцентом на скорость полезных химических реакций (непосредственно связанных с образованием химического осаждения из паровой фазы, контролируемого и регулируемого немаксвелловским распределением электронов по энергии.

Ключевые слова: функция распределения электронов по энергии-ФРЭЭ, моносилан SiH_4, метод Монте-Карло, химическое осаждение из паровой фазы (PECVD), уравнение Больцмана, распределение Максвелла.

References

1 Matsuda A. Microcrystalline silicon. Growth and device application, Journal of Non-Crystalline Solids, 338, 112 (2004).

2 Kushner M.J. A model for the discharge kinetics and plasma chemistry during plasma enhanced chemical vapour deposition of amorphous silicon, Journal of applied physics, 63, 2532-2551 (1988).

3 Wang S. Evolution of a-Si: H to nc-Si: H transition of hydrogenated silicon lms deposited by trichlorosilane using principle component analysis of optical emission spectroscopy, Materials Chemistry and Physics, 240, 122-186 (2020).

4 Raghunath P Lee Y. Ab initio chemical kinetics for reactions of H atoms with SiH_x (x= 13) radicals and related unimolecular decomposition processes, International Journal of Quantum Chemistry, 113, 1735-1746 (2013).

5 Nguyen T.N.,Lee Y.M. Wu J.S.,Lin M.C., Ab Initio Chemical Kinetics for the Thermal Decomposition of SiH_4^+ Ion and Related Reverse Ion Molecule Reactions of Interest to PECVD of a-Si: H Films, Plasma Chemistry and Plasma Processing, 37, 1249-1264 (2017).

6 Phillip J.S Kushner M.J. Monte Carlo simulation of surface kinetics during plasma enhanced chemical vapour deposition of SiO_2 using oxygen/tetraethoxysilane chemistry, Journal of Vacuum Science Technology A: Vacuum, Surfaces, and Films, 11, 2562-2571 (1993).

7 Babahani O., Hadjadj S., Khelfaoui F., Kebaili H. O. Lemkeddem S. Monte Carlo simulation of chemical reactions in plasma enhanced chemical vapour deposition: From microscopic view to macroscopic results, Silicon, 11, 1267-1274 (2019).

8 Balbuena J.P Martin-Bragado I. Lattice kinetic Monte Carlo simulation of epitaxial growth of silicon thin films in H_2/SiH_4 chemical vapour deposition systems, Thin Solid Films, 634, 121-133 (2017).

9 Da B. Lihao Y. Monte Carlo simulation study of reflection electron energy loss spectroscopy of an Fe/Si over layer sample, Surface and Interface Analysis, 52, 742-754 (2020).

10 Kimberly R.M., Alan L.M., Eduardo D.G. Storage of natural gas by adsorption on activated carbon, Chemical engineering science, 47, 1569-1579 (1992).

11 Holt J.K., Swiatek M., Goodwin D.G. Harry A.A. Gas Phase and Surface Kinetic Processes in Hot-Wire Chemical Vapour Deposition, Amorphous Heterogeneous Silicon Thin Films, 609, 62 (2011).

12 Shogo S., Masao S., Hisanao A., Shigeo S. Silicon-Carbon alloy film formation on Si (100) using SiH_4 and CH_4 reaction under low-energy ECR Ar plasma irradiation, Materials Science in Semiconductor Processing, 70, 188-192 (2017).

13 Kushner M.J. A model for the discharge kinetics and plasma chemistry during plasma enhanced chemical vapour deposition of amorphous silicon, Journal of applied physics, 63, 2532-2551 (1988).

14 Benilov M.S. Teoriya elektricheskih zondov v potokah slaboionizovannoj plazmy vysokogo davleniya, Teplofizika vysokih temperatur, Rossijskaya akademiya nauk, Otdelenie energetiki, mashinostroeniya, mekhaniki i . . . [Theory of electric probes in streams of low-ionized high-pressure plasma, Thermophysics of High Temperatures, Russian Academy of Sciences, Department of Power Engineering, Mechanical Engineering, Mechanics and ...], 26, 993-1004 (1988). [in Russian]

15 Kees L., Wim J.G., Ioannis P., Rath K. Ion bombardment measurements and simulations of a low temperature VHF PECVD SiH_4H_2 discharge in the a-Si: H to μc-Si: H transition regime, physics status solidi (a), 213, 1680-1685 (2016).

16 Timothy J.S., Kushner M.J. Monte Carlo-fluid model of chlorine atom production in Cl_2, HCl, and ﬄCCl_4 radio-frequency discharges for plasma etching, Journal of Vacuum Science Technology B: Microelectronics and Nanometer Structures Processing, Measurement, and Phenomena, 10, 2179-2187 (1992).

17 Marvi Z., Xu S., Foroutan G., Ostrikov K., Levchenko I. Plasma-deposited hydrogenated amorphous silicon films: multi scale modelling reveals key processes, RSC advances, 7, 19189-19196 (2017).

18 Tawara H., Itikawa Y., Nishimura H., Yoshino M. Cross sections and related data for electron collisions with hydrogen molecules and molecular ions, Journal of Physical and Chemical Reference Data, 19,617-636 (1990).

19 Timothy J.S. Monte Carlo-fluid hybrid model of the accumulation of dust particles at sheath edges in radio-frequency discharges, Applied physics letters, 59, 638-640 (1991).

20 Sasa D., Zoran M.R., Ronald D.W., Toshiaki M., Zoran L.P. Monte Carlo analysis of ionization effects on spatio-temporal electron swarm development, The European Physical Journal D, 68, 166 (2014).

21 Zhang B. Zhang X. Electron energy distribution functions relevant for weakly ionized SiH_4H_2 plasma, Journal of Physics D: Applied Physics, 53, 115-201 (2020).

22 Jason P. Modeling and Experimental process optimization for a $SiH_4 + H_2$ surface wave plasma discharge for silicon photovoltaic, (2014).

23 Grari M. Zoheir C. Numerical Modeling of Non-equilibrium Plasma Discharge of Hydrogenated Silicon Nitride ($SiH_4/NH_3/H_2$), International Journal of Engineering, 33, 1440-1449 (2020).
24 Hagelaar G.J. Pitchford L.C. Solving the Boltzmann equation to obtain electron transport coefficients and rate coefficients for fluid models, Plasma Sources Science and Technology, 14, 722 (2005).
25 Oblapenko G., Goldstein D., Varghese P. Moore C. A velocity space hybridization-based Boltzmann equation solver, Journal of Computational Physics, 408, 109-302 (2020).
26 Mohammad M.O., Saeed R.H. Boltzmann equation studies on electron swarm parameters for oxygen plasma by using electron collision cross sections, Zanco Journal of Pure and Applied Sciences, 32, 36-53 (2020).
27 Chapman S., Thomas G.C. David B. The mathematical theory of non-uniform gases: an account of the kinetic theory of viscosity, thermal conduction and diffusion in gases (Cambridge: Cambridge university press, 1990, 423 p.).
28 Holstein T. Energy distribution of electrons in high frequency gas discharges, Physical Review, 70, 367 (1946).
29 Gryzinski M. Classical theory of atomic collisions. I. Theory of inelastic collisions, Physical Review, 138, A336 (1965).
30 Guyot J., Miley G. Verdeyen J. Application of a two-region heavy charged particle model to Noble-gas plasmas induced by nuclear radiations, Nuclear Science and Engineering, 48, 373-386 (1972).
31 Tsendin L. The electron diffusion coefficient in energy in bounded collisional plasmas, IEEE transactions on plasma science, 34, 728-737 (2006).
32 Bogaerts A., Eckert M., Mao M. Neyts E. Computer modelling of the plasma chemistry and plasma-based growth mechanisms for nano structured materials, Journal of Physics D: Applied Physics, 44, 174030 (2011).
33 King H., Pflug A., Ortner K., Hofer M., Harig T., Sittinger V. DSMC - Simulation of the influence of hydrogen addition on the properties of silicon deposited by HWCVD, Surface and Coatings Technology, 379, 125035 (2019).

Information about authors:

Кунаков С.К. - ***негізгі автор***, Ядролық және теоретикалық физика кафедрасының профессоры,Әль-Фараби атындағы ұлттық университеті, 71, Алматы, Қазақстан.

Имаш Ә.А. - инженерлiк физика кафедрасының «7M05301 -Қолданбалы және инженерлiк физика» мамандығы бойынша магистранты, Қ.И.Сәтпаева атындағы Қазақ Ұлттық Техникалық Зерттеу Университетi,Сатпаева көшесi, 22а, Алматы, Қазақстан

Kunakov S.K. - ***The main author***, Professor of the Department of Nuclear and Theoretical Physics, Al-Farabi Kazakh National University, 71 avenue Al-Farabi, Almaty, Kazakhstan.

Imash A.A. - Master's student in "7M05301 Applied and Engineering Physics" of the Department of Engineering Physics, K.I. Satpayev Kazakh National Technical Research University, 22a Satpayev Ave., Almaty, Kazakhstan.